microbial biotechnology

Open Access

Biotechnological production optimization of argyrins – a potent immunomodulatory natural product class

Domen Pogorevc[1,2,3] and Rolf Müller[1,2,3,*]

[1]*Helmholtz Centre for Infection Research, Helmholtz Institute for Pharmaceutical Research Saarland (HIPS), Saarland University Campus, Saarbrücken, 66123, Germany.*

[2]*Department of Pharmacy, Saarland University, Saarbrücken, 66123, Germany.*

[3]*DZIF – German Centre for Infection Research, Partnersite Hannover-Braunschweig, Braunschweig, Germany.*

Summary

Argyrins represent a family of cyclic octapeptides exhibiting promising immunomodulatory activity *via* inhibiting mitochondrial protein synthesis, which leads to reduced IL-17 production by the T-helper 17 cells. Argyrins are formed by a non-ribosomal peptide synthetase (NRPS), originating from the myxobacterial producer strains *Archangium gephyra* Ar8082 and *Cystobacter* sp. SBCb004. In this work, a previously established heterologous production platform was employed to provide evidence of direct D-configured amino acid incorporation by the argyrin assembly line. An adenylation domain of the argyrin NRPS was characterized and shown to have a high preference for D-configured amino acids. Eight novel argyrin derivatives were generated *via* biosynthetic engineering of the heterologous production system. The system was also optimized to enable formation of methylated argyrin C and D derivatives with improved immunosuppressive activity compared with their unmethylated counterparts. Furthermore, the optimization of cultivation conditions allowed exclusive production of one major derivative at a time, drastically improving the purification process. Importantly, engineering of transcription and translation initiation resulted in a substantially improved production titre reaching 350–400 mg l^{-1}. The optimized system presented herein thus provides a versatile platform for production of this promising class of immunosuppressants at a scale that should provide sufficient supply for upcoming pre-clinical development.

Received 9 September, 2021; revised 13 October, 2021; accepted 14 October, 2021.

*For correspondence. E-mail Rolf.Mueller@helmholtz-hips.de; Tel. +49 681 988063002; Fax +49 681 988063009.

Microbial Biotechnology (2021) **0**(0), 1–17
doi:10.1111/1751-7915.13959
Funding Information
This work was supported by DZIF.

Introduction

Natural product-based immunosuppressive agents have been used for decades in human medical applications, e.g., to prevent organ rejections after transplantation. Among various compound classes with immunomodulatory activity, the best known examples are cyclosporine (Canafax and Ascher, 1983), FK506 (Wallemacq and Reding, 1993) and rapamycin (Dumont and Su, 1995), the latter approved for application in humans by the FDA in 1999 (Mann, 2001). Recent results have highlighted the importance of argyrins, identifying them as non-competitive inhibitors of the human immunoproteasome (Allardyce and Bell, 2019). They were also shown to exhibit strong immunosuppressive activity by targeting the mitochondrial elongation factor (EF-G1) in yeast and mammalian cells, thereby reducing the IL-17 production by the human T-helper 17 cells (Almeida *et al.*, 2021). In addition to the immunosuppressive activity, argyrin A induces apoptosis and blocks angiogenesis by preventing the destruction of the cyclin kinase inhibitor p27kip1 through proteasome inhibition (Nickeleit *et al.*, 2008; Stauch *et al.*, 2010). Those properties highlight the potential of argyrins as promising immunomodulatory drug candidates.

Argyrins are a family of cyclic octapeptides produced by the myxobacterial strains, *Archangium gephyra* Ar8082 and *Cystobacter* sp. SBCb004. Biosynthetically they are generated from amino acids by a non-ribosomal peptide synthetase (NRPS) (Pogorevc *et al.*, 2019b). NRPSs represent large multifunctional megasynthetases involved in the biosynthesis of numerous structurally diverse compounds, among them several marketed drugs, e.g., penicillin, vancomycin and cyclosporine (Finking and Marahiel, 2004; Süssmuth and Mainz, 2017). The corresponding genes, encoding the production machinery for the biosynthesis of a particular compound family, are usually clustered within the chromosome of the microbial producer strain and are referred to as the corresponding biosynthetic gene

cluster (BGC). The Argyrin BGC from *Cystobacter* sp. SBCb004 consists of one operon including the five genes *arg12345* (Pogorevc *et al*., 2019b). The genes *arg2* and *arg3* encode the two large NRPS subunits responsible for the biosynthesis of the core structure. *arg1* encodes a radical *S*-adenosyl-L-methionine (SAM)-dependent methyltransferase catalysing the *C*-methylation of the second L-tryptophan and *arg5* and *arg4* encode a tryptophan-2,3-dioxygenase and an *O*-methyltransferase responsible for oxygenation and subsequent *O*-methylation of the same L-tryptophan respectively (Fig. 1).

Although total synthesis approaches have already been developed for the generation of argyrins and novel derivatives (Ley and Priour, 2002; Bülow *et al*., 2010; Chen *et al*., 2014), the establishment of more efficient and cost-effective supply routes is highly demanded to further investigate and develop this promising compound class. The BGC from *Cystobacter* sp. SBCb004 was recently used as a template for the development of a synthetically engineered heterologous production platform based on *Myxococcus xanthus* DK1622*ΔmchA-tet* as host organism, allowing further exploitation of argyrins and novel derivatives thereof. This led to the identification of novel argyrin derivatives and enabled combined production titres of argyrins A and B up to 160 mg l^{-1} (Pogorevc *et al*., 2019b).

In this work, we optimized the previously reported heterologous production system by genetic engineering approaches to manipulate the transcription and translation initiation which led to an improved total argyrin production titre of 350–400 mg l^{-1}. Importantly, we were able to direct the biosynthesis towards the production of single analogues with improved pharmaceutical properties. Coexpression of *arg1* or *arg451* led to heterologous production of methylated argyrins C/D, which were recently shown to exert improved immunosuppressive properties, compared with argyrins A/B (Almeida *et al*., 2021). Furthermore, engineering of the argyrin production profile enabled exclusive production of specific argyrin derivatives and thus drastically simplified the purification process.

Results and discussion

Argyrin production profile engineering

Production of argyrins C and D by coexpression of the radical SAM methyltransferase Arg1. The *arg1* gene was excluded from the argyrin BGC in our previous study (Pogorevc *et al*., 2019b) to simplify the production profile and avoid inefficient methylation by Arg1. In light of the novel immunomodulatory activities described for methylated argyrins (Almeida *et al*., 2021), we aimed to further improve the production of the methylated argyrin variants, such as argyrins C and D. Therefore, an

Argyrins

	R_1	R_2	R_3	R_4
A	CH_3	CH_3	H	OCH_3
B	CH_2CH_3	CH_3	H	OCH_3
C	CH_3	CH_3	CH_3	OCH_3
D	CH_2CH_3	CH_3	CH_3	OCH_3
E	CH_3	CH_3	H	H
F	CH_3	CH_2OH	H	OCH_3
G	CH_2CH_3	CH_2OH	H	OCH_3
H	CH_3	H	H	OCH_3
I	CH_2CH_3	CH_3	H	H
J	CH_2CH_3	H	H	OCH_3
F3	CH_3	CH_2OH	H	H
G3	CH_2CH_3	CH_2OH	H	H
N	CH_2CH_3	CH_2OH	CH_3	OCH_3
N3	CH_2CH_3	CH_2OH	CH_3	H
M	CH_3	CH_2OH	CH_3	OCH_3
M3	CH_3	CH_2OH	CH_3	H
O	CH_2CH_3	CH_3	CH_3	H
P	CH_3	CH_3	CH_3	H
R	CH_2CH_3	H	CH_3	OCH_3
S	CH_3	H	CH_3	OCH_3

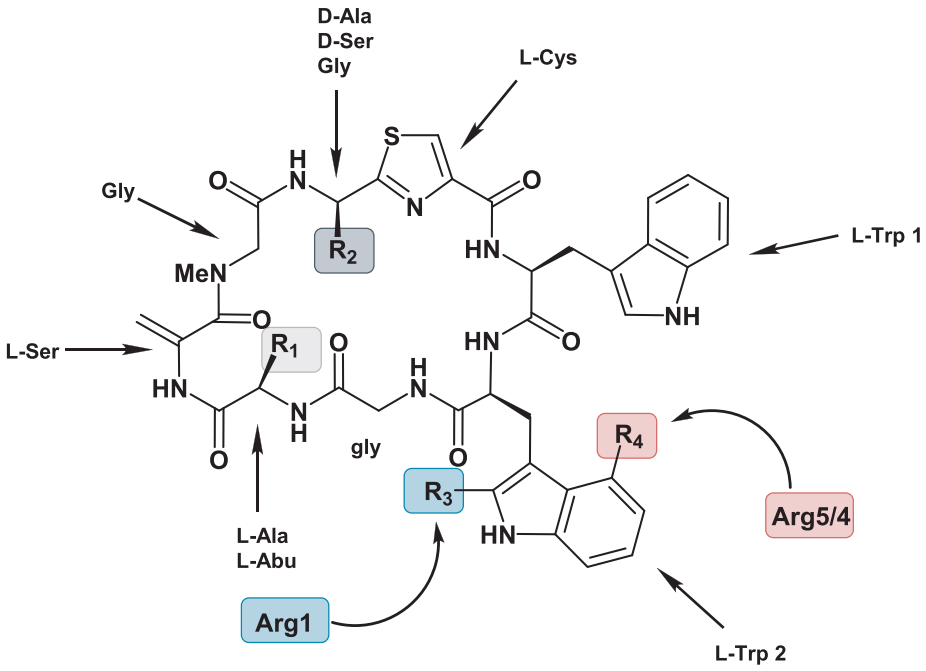

Fig. 1. The argyrin core structure with highlighted amino acid substrates as they are incorporated by the corresponding NRPS modules. The structural diversity is introduced by the promiscuous NRPS modules (R_1 and R_2) and the highlighted tailoring enzymes Arg1, Arg4 and Arg5 (R_3 and R_4).

expression vector for coexpression of the gene encoding the radical-SAM methyltransferase Arg1 in the heterologous argyrin producer *Mx.* DK1622::pArg2345 (see Table S4 for full strain names) was designed. A previous gene miss-annotation came to our attention which led to an extensive *in silico* analysis of the native producer's (*Cystobacter* sp. SBCb004) genome sequence using FramePlot (Ishikawa and Hotta, 1999) and Basic Local Alignment Search Tool (BLAST) (Altschul *et al.*, 1990) to correctly re-annotate the *arg1* gene sequence (see Experimental procedures). The identified missing piece of the *arg1* gene was PCR amplified and cloned into the pGH-arg1-V1 plasmid obtained from a gene synthesis company. After subcloning of the reconstituted *arg1* into the expression vector, the construct was integrated into the genome of *Mx.* DK1622::pArg2345 *via* homologous recombination and the production profile of *Mx.* DK1622::pArg2345-arg1 was verified. HPLC-MS analysis revealed similar production rates of argyrins A and B based on the MS peak area in the control strain and the mutant harbouring the *arg1* gene copy (Fig. 2). Notably, the coexpression of *arg1* led to the production of argyrins C and D as minor derivatives (Fig. 2). To investigate if the methylation efficiency can be improved to increase the conversion rate of argyrins A and B into their methylated counterparts (argyrins C and D), the production medium was supplemented with vitamin B_{12}, an essential co-factor for radical-SAM enzymes (Pierre *et al.*, 2012; Zhang and van der Donk, 2012; Kim *et al.*, 2013). The HPLC-MS analysis indeed revealed a full conversion of argyrins A and B into argyrins C and D respectively (Fig. 2).

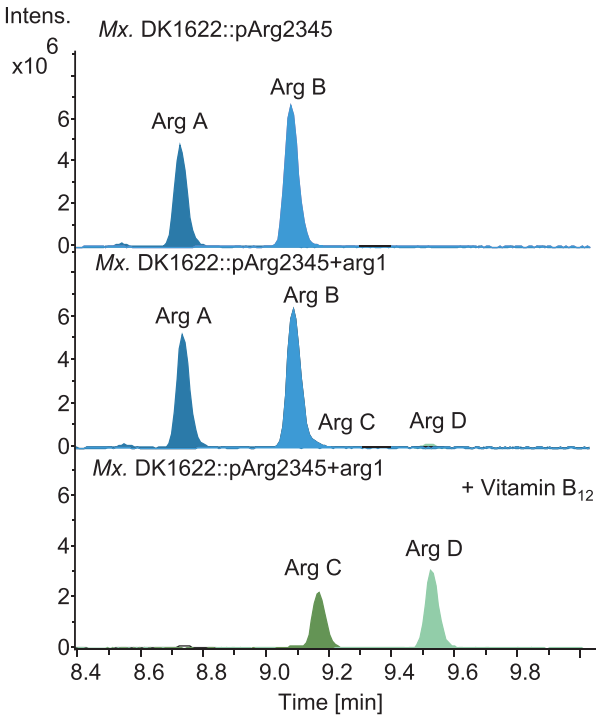

Fig. 2. Conversion of argyrins A and B into C and D after coexpression of *arg1* in *Mx.* DK1622::pArg2345 and further improvement of argyrins C and D production by addition of vitamin B_{12}. HPLC-MS analysis of the fermentation broth extracts showing extracted ion chromatograms (EICs) $[M + H]^+ = 825.313$ (Arg A), $[M + H]^+ = 839.329$ (Arg B), $[M + H]^+ = 839.329$ (Arg C) and $[M + H]^+ = 853.344$ (Arg D). The full mutant names were abbreviated (see Table S4).

Argyrin production profile engineering by cultivation condition optimization. The high structural diversity of argyrins is caused by the tailoring reactions catalysed by Arg1, Arg4 and Arg5, combined with the relaxed substrate tolerance of the first and fourth modules of the NRPS. A complex mixture of numerous derivatives, produced by the native or the heterologous producers, poses a downstream processing challenge when trying to produce a specific derivative with high purity. We applied extensive medium optimization to decrease the number of produced derivatives and thus simplify the future purification process. The heterologous argyrin producer yields about the same amount of argyrins A and B when cultivated in CTT medium. In contrast, it has previously been noticed that the argyrin production profile shifts substantially in favour of argyrin A when the *Mx.* DK1622::pArg2345 is cultivated in M7/s4 medium, probably due to the low external supply of L-α-aminobutyric acid (L-Abu) (Fig. 3A) (Pogorevc *et al.*, 2019b). We were able to shift the production rate between argyrins A and B by cultivating the heterologous argyrin producer *Mx.* DK1622::pArg2345 in different media and/or by supplementing with 10mM L-Abu. This led to a shift in the production profile towards a near exclusive production of argyrin B (Fig. 3A), supporting the hypothesis of a low external L-Abu supply. This also indicates that the assembly line prefers incorporation of L-Abu over L-alanine, to yield argyrin B rather than argyrin A. To show that the shift from argyrin C to argyrin D can also be achieved by the supplementation of L-Abu, the same cultivation experiments were performed while coexpressing the *arg1* leading to a near exclusive production of argyrin D (Fig. 3B).

Evaluation of different promoter-5'-UTR systems and their impact on the argyrin production level

Promoters are the key regulators of gene expression that have the potential to increase or decrease secondary metabolite production levels (Ongley *et al.*, 2013). There are only a handful of promoter systems which were successfully used for gene expression in

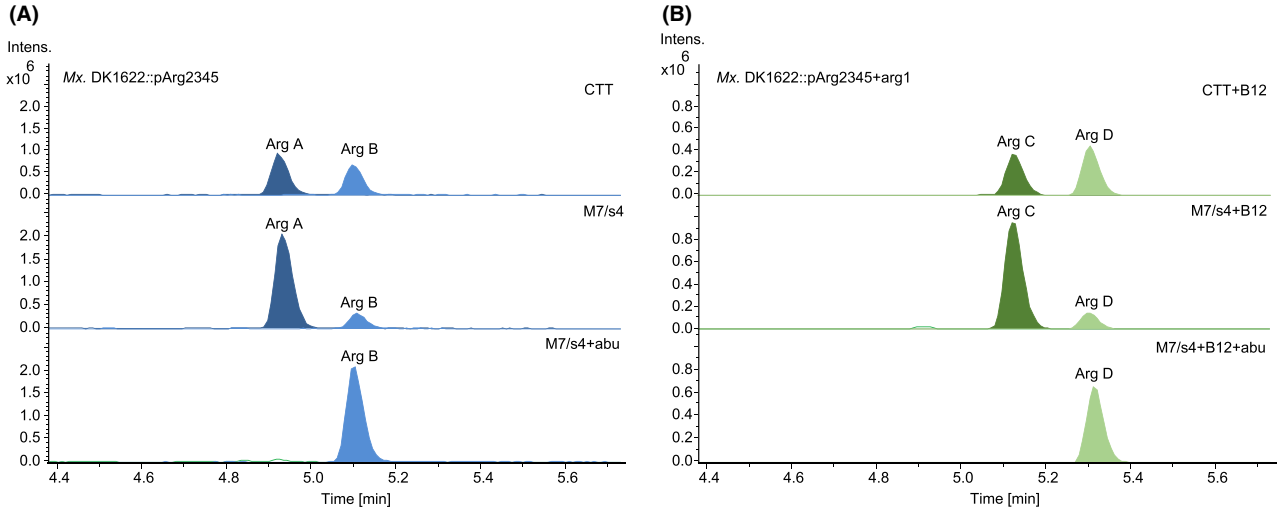

Fig. 3. Argyrin production profile engineering through medium/cultivation optimization and *arg1* coexpression. Variation in production of argyrins A and B in different media (A). Variation in production of argyrins C and D in different media (B). HPLC-MS analysis of supernatant showing EICs $[M + H]^+$ = 825.313 (Arg A), $[M + H]^+$ = 839.329 (Arg B), $[M + H]^+$ = 839.329 (Arg C) and $[M + H]^+$ = 853.344 (Arg D). The full mutant names were abbreviated (see Table S4).

myxobacteria, including P_{nptII}, P_{tet}, P_{pm} and P_{van} (Table S2). Most of those systems were initially developed and evaluated in different non-myxobacterial host organisms and were later established in myxobacteria due to a lack of highly efficient myxobacterial promoters. P_{nptII} and P_{van} are commonly used for the activation of silent BGCs in terms of genome mining and also for heterologous BGC expression (Table 1). Besides the P_{IPTG}, the P_{van} is the only viable option for inducible gene expression (Iniesta *et al*., 2012). Notably, no other reliable inducible promoters were described for myxobacteria so far (Perlova *et al*., 2006). Since there was no available data for direct comparison of the gene expression or secondary metabolite production by BGCs driven by the aforementioned promoters in myxobacteria, we decided to test all commonly used promoter systems and evaluate their direct effect on the production level of argyrins with a high production titre being the main priority.

The promoter harbouring constructs were designed based on the four different promoter systems P_{nptII}, P_{van}, P_{pm} and P_{tet}. For P_{van} and P_{tet}, we designed versions with and without repressor gene, resulting in a total of six new synthetic promoters. To minimize the translational influence of the native 5'-untranslated regions (5'-UTRs) downstream of each promoter, a synthetically engineered 5'-UTR optimized for high expression in *M. xanthus* DK1622 was designed *in silico*. This synthetic 5'-UTR was used instead of the native 5'-UTR region in all six designed promoter harbouring constructs which were generated by DNA synthesis. A detailed overview of the promoter fragments is illustrated in Fig. S3 and described in Experimental procedures.

The original P_{nptII} from the pArg2345-V1-BsaI construct was exchanged *via* restriction hydrolysis and DNA ligation with the six synthesized promoter sequences. The generated expression constructs with the different promoter-5'-UTRs (see Experimental procedures) were transferred into *M. xanthus* DK1622*ΔmchA-tet* and integrated into the genome via homologous recombination. The cultivation of the generated strains was performed in M7/s4 medium supplemented with respective argyrin precursor amino acids to reduce the negative impact on the production caused by the lack of nutrients. It was previously shown that the argyrin production titre in amino acid supplemented M7/s4 medium increases substantially compared with the CTT or M7/s4 medium without amino acid supplementation (Pogorevc *et al*., 2019b). HPLC-MS analysis of the fermentation extracts revealed that argyrins were indeed produced by all mutants, however, with substantial differences in the production levels depending on the promoter system. In this cultivation experiment, the supplementation with the amino acid mixture also increased the production of the previously described argyrin I, a derivative lacking the methoxy group introduced by the Arg5 and Arg4 enzymes (Fig. 1) (Pogorevc *et al*., 2019b).

Quantification of argyrins A, B and I revealed that the highest total argyrin production and an increase by about 40%, compared with the control, was achieved with the use of P_{nptII} after exchanging the native 5'-UTR with the synthetic one. This indicates that an efficient translation process was probably the bottleneck in the control system (Fig. 4). The expression of the argyrin BGC regulated by $P_{tetΔR}$ and $P_{vanΔR}$ resulted in higher argyrin production levels compared with the control system with

Table 1. Heterologous production of PKS/NRPS-derived natural products in *M. xanthus*.

Compound	Native producer	Pathway type [size]	Promoter	Yield[a]	Ref
Alkypyrones	*MCy9487*	PKS [6 kb]	P_{van}	n.d.	Hug *et al.* (2019)
Argyrins A, B, I	*Cystobacter* sp. SBCb004	NRPS [33 kb]	P_{nptII}	230 mg l^{-1}	Pogorevc *et al.* (2019b)
Argyrins A, B, I	*Cystobacter* sp. SBCb004	NRPS [33 kb]	P_{nptII}	350–400 mg l^{-1}	This study
Argyrins A, B, I	*Cystobacter* sp. SBCb004	NRPS [33 kb]	P_{van}	300 mg l^{-1}	This study
Argyrins A, B, I	*Cystobacter* sp. SBCb004	NRPS [33 kb]	$P_{van\Delta R}$	250–300 mg l^{-1}	This study
Argyrins A, B, I	*Cystobacter* sp. SBCb004	NRPS [33 kb]	P_{tet}	50–100 mg l^{-1}	This study
Argyrins A, B, I	*Cystobacter* sp. SBCb004	NRPS [33 kb]	$P_{tet\Delta R}$	200–250 mg l^{-1}	This study
Argyrins A, B, I	*Cystobacter* sp. SBCb004	NRPS [33 kb]	P_{pm}	200 mg l^{-1}	This study
Bengamide	*Myxococcus virescens*	PKS/NRPS [25 kb]	P_{nptII}	> 10 mg l^{-1}	Wenzel *et al.* (2015)
Corallopyronin A	*Corallococcus coralloides*	PKS/NRPS [65 kb]	P_{nptII}	37 mg l^{-1}	Sucipto *et al.* (2017)
Corallopyronin A	*Corallococcus coralloides*	PKS/NRPS [65 kb]	P_{van}	100 mg l^{-1}	Pogorevc *et al.* (2019a)
Cystobactamide Cys919-1	*Cystobacter velatus* Cbv34	NRPS [52 kb]	P_{van}	8.1 mg l^{-1}	Groß *et al.* (2021)
Dawenol	*Stigmatella aurantiaca*	PKS [21 kb]	Native	n.d.	Oßwald *et al.* (2014)
Disorazol A_2	*Sorangium cellulosum* So ce12	PKS/NRPS [58kb]	P_{tet}/P_{cp25}	~ 1 mg l^{-1}	Tu *et al.* (2016)
Epothilone	*Sorangium cellulosum*	PKS/NRPS [56 kb]	Native	0.1–0.4 mg l^{-1}	Julien and Shah (2002); Lau *et al.* (2002); Oßwald *et al.* (2014)
Haliangicin	*Haliangium ochraceum* SMP-2	PKS [47.8 kb]	Native	11 mg l^{-1}	Sun *et al.* (2016)
Myxochromide A	*Myxococcus xanthus*	PKS/NRPS [29 kb]	P_{nptII}	~ 500 mg l^{-1}	Yan *et al.* (2018b)
Myxochromide S	*Stigmatella aurantiaca*	PKS/NRPS [29 kb]	P_{nptII}	> 500 mg l^{-1}	Fu *et al.* (2008)
Myxopyronin A	*Myxococcus fulvus*	PKS/NRPS [53 kb]	P_{nptII}	156 mg l^{-1}	Sucipto *et al.* (2017)
Myxothiazol	*Stigmatella aurantiaca*	PKS/NRPS [57 kb]	P_{pm}	20 mg l^{-1}	Perlova *et al.* (2006)
Oxytetracycline	*Streptomyces rimosus*	PKS [32 kb]	Native	10 mg l^{-1}	Stevens *et al.* (2010)
Pretubulysin	*Cystobacter* sp.	PKS/NRPS [40 kb]	P_{tet}	0.2 mg l^{-1}	Chai *et al.* (2012)
PUFAs[b]	*Aetherobacter fasciculatus*	PKS/FAS [18 kb]	P_{tet}	~ 1 mg CDW^{-1}	Gemperlein *et al.* (2014)
Pyxidicyclines	*Pyxidicoccus fallax* And48	PKS [33 kb]	P_{van}/P_{nptII}	n.d.	Panter *et al.* (2018)
Vioprolide B, D	*Cystobacter violaceus*	NRPS [56 kb]	P_{tet}	80 mg l^{-1}	Yan *et al.* (2018a)

n.d., not determined.
a. Based on shake flask experiments.
b. Polyunsaturated fatty acids.

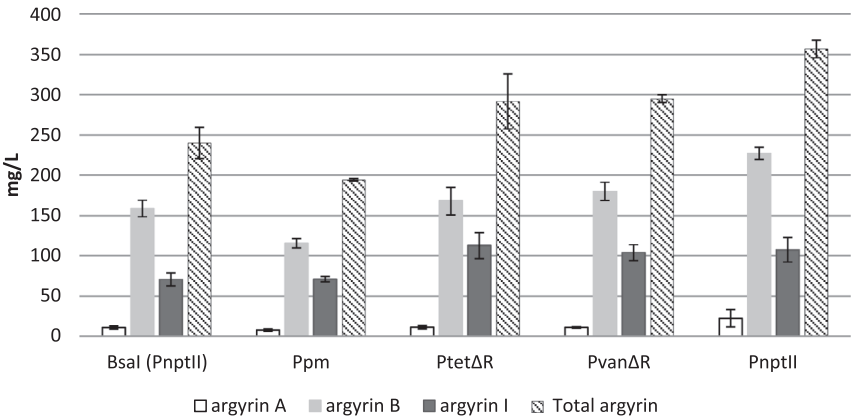

Fig. 4. Production levels of argyrins A, B and I evaluated in heterologous argyrin producers with different promoter systems in comparison with control (PnptII-native 5'UTR). Samples were analysed by HPLC-MS, and the production titres of argyrins A, B and I, as well as the total argyrin amount, were quantified as described in Experimental procedures.

P_{nptII} and the native 5'-UTR sequence. The lowest production was achieved by the P_{pm}, which, despite the optimized 5'-UTR region, resulted in a lower argyrin production than observed in the control (Fig. 4).

Second, we evaluated the production by the mutants harbouring the argyrin BGC controlled by the inducible promoter systems (P_{tet} and P_{van} with the respective repressor genes), under induced and uninduced conditions. The versions of $P_{tet\Delta R}$ and $P_{van\Delta R}$ without repressor were also evaluated in parallel, without addition of inducers, to allow direct comparison.

The induction of the P_{tet} with tetracycline did not result in increased production levels; however, the deletion of the repressor gene in $P_{tet\Delta R}$ led to a significant increase in argyrin production titre (Fig. 5). This hints that the induction of the P_{tet} system in *M. xanthus* DK1622 is not

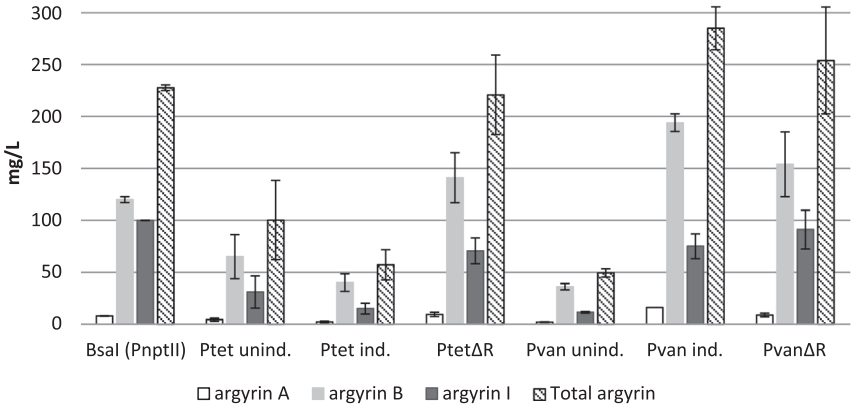

Fig. 5. Production levels of argyrins A, B and I evaluated in heterologous argyrin producers with different promoter systems. The yields detected in mutants harbouring the argyrin BGC under the control of P_{tet} or P_{van} were evaluated under induced and uninduced conditions. Repressor deletion mutants and control (PnptII-native 5'UTR) were evaluated under uninduced conditions. Samples were analysed by HPLC-MS and production titres of argyrins A, B and I were quantified as described in Experimental procedures.

working efficiently. As expected, in case of the P_{van}, the induction with 1 mM vanillate led to a near sixfold increase in production of argyrin compared with the uninduced control, reaching a similar production titre as achieved by the $P_{van\Delta R}$ (Fig. 5). It appears that deletion of repressors in P_{tet}- and P_{van}-inducible promoter systems has no negative effect on the argyrin production titre. Promoters without repressors can thus be used to simplify argyrin production and eliminate the need for supplementation with inducers. Notably, argyrins do not appear to be auto-toxic to the producer strain at the observed production titres. The attempt to evaluate the MIC at 650 mg l^{-1} of argyrin B resulted in argyrin precipitation and growth of *M. xanthus* cells on the argyrin precipitate. This correlates with our *in silico* analysis which showed that the exchange of S459 in the argyrin susceptible EF-G of *Pseudomonas aeruginosa* with an R459 (found at this position in the EF-G of *M. xanthus*) could lead to a significant clash and thereby prevent binding of argyrin B to the EF-G of *M. xanthus* (Figs S5 and S6). However, the presence of repressors should be re-evaluated for use in different, especially uncharacterized, secondary metabolite BGCs as the produced compounds could exert auto-toxicity towards the producer strain. In such cases, inducible promoters can prove advantageous since they at least enable the detection of the auto-toxic factor after the induction of the BGC of interest and in some cases allow production of the toxic metabolite in the presence of an adsorbent resin (Panter *et al.*, 2018).

From the results we conclude that the highest argyrin production titre was achieved upon expression of *arg2345* under the control of the synthetic 5'-UTR and the P_{nptII}, with the $P_{tet\Delta R}$ and $P_{van\Delta R}$ providing slightly lower argyrin production titres. A similar production titre was achieved with the induced P_{van} in the presence of *vanR*. These results might serve as an orientation for future experiments to increase the production titre of other myxobacterial secondary metabolites. However, in addition to the promoter efficiency, the 5'-UTR region can have a significant effect on protein expression (Dvir *et al.*, 2013) influencing metabolite titres, as it was shown in this study. The improved production system generated in this study reaches a combined total production of argyrins at 350–400 mg l^{-1} and ranks with the most successful examples in heterologous expression studies on myxobacterial megasynthetases in *M. xanthus* (Table 1). We also attempted to further improve the argyrin production titre by expressing two copies of the same argyrin BGCs in one heterologous producer strain. However, the growth of the resulting mutant strains was inconsistent in these experiments and the results showed no obvious advantage of expressing two BGCs over a single BGC copy where stability of the genotype might be a complicating factor (data not shown).

Resolving the biosynthetic tailoring bottleneck

As mentioned above, supplementation of M7/s4 medium with amino acids led to a significant increase in total argyrin production including the titre of argyrin I, the non-tailored precursor of argyrin B. This indicates that the catalytic capability of Arg5 (tryptophan-2,3-dioxygenase) and Arg4 (hydroxyindole O-MT) reaches a limit where no more argyrin can be modified. To facilitate conversion of argyrin I to its methoxylated counterparts (argyrin B or D) we generated and overexpressed two separate expression constructs harbouring additional copies of the tailoring genes (*arg45* or *arg451* operons) regulated by P_{nptII} in *Mx*. DK1622::pArg2345. The expression constructs were integrated into the host genome *via* the mx8 phage integrase. The HPLC-MS analysis of the *Mx*.

DK1622::arg2345-arg45 production profile revealed almost complete conversion of argyrin I to argyrin B (Fig. 6). Coexpression of the *arg451*, on the other hand, revealed a complete conversion of argyrin I to argyrin B; however, not all argyrin B could further be methylated to argyrin D by a single copy of *arg1* (Fig. 6). Additionally, after a visual inspection of the respective crude extracts we have observed a high degree of precipitation in the samples produced by the strains harbouring the *arg1* gene copy. We thus assumed that argyrin D is poorly soluble in methanol. Consequently, the methanol-dissolved crude extracts were dried and re-dissolved in the same volume of DMSO, which resulted in no observable precipitate and indeed in a subsequent apparent increase in argyrin D was detected in the MS (Fig. S4).

Explaining the origin of D-configured amino acids incorporated by the fourth module

As previously reported, the alanine (resulting in $R_2 = CH_3$ as shown in Fig. 1) and serine ($R_2 = CH_2OH$) units incorporated by the fourth module of the argyrin NRPS exhibit D-configuration in mature argyrin derivatives. According to the currently known argyrins, alanine seems to be the preferred substrate, whereas serine and glycine ($R_2 = H$) were only observed in minor derivatives. In most D-amino acid-containing non-ribosomal peptides, L-configured amino acids are initially activated by the A domain and subsequently epimerized by a downstream E domain or a dual condensation–epimerization domain (Marahiel and Stachelhaus, 1997; Rausch *et al*., 2007). This seems to also be the case in the first module of the argyrin NRPS, which activates an L-amino acid substrate, epimerizes it by the action of the epimerization (E) domain and subsequently processes it by the downstream D-specific C domain [$_DC_L$ type according to Rausch *et al*. (Rausch *et al*., 2007)]. D-amino acid–activating A domains are thus uncommon or poorly characterized as only a few cases have been reported thus far (Wu *et al*., 1987; Shi *et al*., 2016; Kaniusaite *et al*., 2021). In a recent study, five A domains located upstream of an E domain in the assembly line were shown to exert the ability to activate D-configured amino acids *in vitro* (Kano *et al*., 2019). In contrast to the first module of the argyrin NRPS, the fourth module does not harbour an E domain for the generation of a D-configured substrate from an A domain-activated L-amino acid. Thus, the origin of D-configured amino acids at the fourth position in the argyrin structure remained unresolved and it was previously hypothesized that the downstream C domain could be responsible for their epimerization. However, this assumption could not be supported by *in silico* analysis according to Rausch *et al*. (Rausch *et al*., 2007) as the characteristic C domain motifs present in the C domains required for generation and/or processing of D-configured amino acids could not be identified (Pogorevc *et al*., 2019b). Due to the superior solubility of D-serine-containing argyrin derivatives and the resulting advantageous pharmaceutical properties, the elucidation of this biosynthetic step remained of high interest.

We aimed to test if D-configured amino acids are directly accepted by the A domain of the fourth module in the argyrin NRPS, rather than L-configured amino acids being incorporated and subsequently epimerized. Since D-serine-containing argyrins are produced as minor derivatives, we assumed that supplementation of the medium with D-serine might boost their production in case D-serine is directly incorporated. To this end, the strains *Mx*. DK1622::pArg2345 and *Mx*. DK1622::pArg2345-arg1 were cultivated in production media (M7/s4 supplemented with argyrin precursor amino acids) supplemented with either L-serine or D/L-serine. HPLC-MS and MS/MS analyses of the culture extracts showed a significant increase in production of D-Abu ($R_1 = CH_2CH_3$) and D-serine ($R_2 = CH_2OH$) containing argyrin derivatives G and G3, for strains cultivated in the

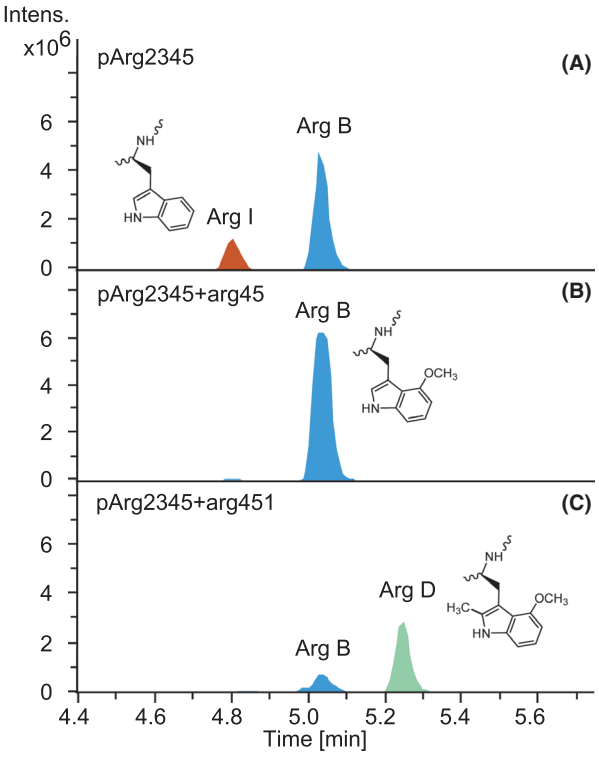

Fig. 6. Production profiles of the producer strains. *Mx*. DK1622::pArg2345 (A), after coexpression of *arg45* (B) and after coexpression of *arg451* (C). HPLC-MS analysis of the crude extracts showing EICs $[M + H]^+ = 839.329$ (Arg B), $[M + H]^+ = 809.318$ (Arg I) and $[M + H]^+ = 853.344$ (Arg D). The full names of the mutant strains were abbreviated (see Table S4).

D/L-serine supplemented medium compared with the strains cultivated in L-serine supplemented medium (Fig. 7 and Table S5). It is therefore likely that the D-configured amino acids are directly incorporated by the fourth module of the argyrin NRPS, which would explain the absence of the epimerization domain in this module (Pogorevc *et al*., 2019b). However, the required isomerase in the natural producer remains unknown (see below). Cultivation of *Mx*. DK1622::pArg2345-arg1 led to the detection of the novel argyrins N and N3 (Fig. 7), which carry an additional methyl group introduced by Arg1, compared with argyrins G and G3, as confirmed by the MS^2 fragmentation (Table S5). Even though the argyrins N and N3 were not detected before, we also searched for them in the extract of the *Mx*. DK1622::pArg2345-arg1 cultivated in the L-serine supplemented medium. We indeed found very low amounts based on the MS peak intensity (Fig. 7). Cultivation in M7/s4 medium without addition of L-Abu, but with supplementation of D-serine, resulted in the detection of the L-alanine ($R_1 = CH_3$) and D-serine ($R_2 = CH_2OH$) containing argyrins M and M3 after HPLC-MS analysis of the respective crude extracts (Table S5). Furthermore, the coexpression of *arg1*, medium variation and high production titres in this experiment led to increased production and detection of additional novel methylated argyrins O, P, R and S as confirmed by the MS^2 fragmentation (Table S5).

To gain more insight into the specificity of the A domain responsible for the activation of the fourth module intermediates, we expressed the corresponding A-PCP part of the Arg3 protein in *E. coli*. We then performed an *in vitro* characterization of the A domain using the malachite green phosphate assay according to the manufacturers protocol and as described by McQuade *et al*. (2009) as well as *in vitro* loading of the PCP domain and analysis by HPLC-MS. The analysis revealed that the A domain is highly specific for D-alanine and slightly less for D-serine, whereas L-configured amino acids were activated very poorly and only after an extended period of time (Fig. S8). Next, we performed *in vitro* loading assays by incubation of the A-PCP bidomain with L-alanine, L-serine, D-alanine, D-serine or glycine and analysed the results by protein MS (Fig. 8). When performing the reaction with 100 μM final amino acid concentration, we observed loading of D-alanine and D-serine (Fig. 8C,E), whereas L-alanine, L-serine or glycine loading could not be observed. Interestingly, we also detected double loading of the D-alanine (Fig. 8C), which was very surprising. This phenomenon of dual activity of an A domain, performing amino acid activation and amide bond formation, has previously

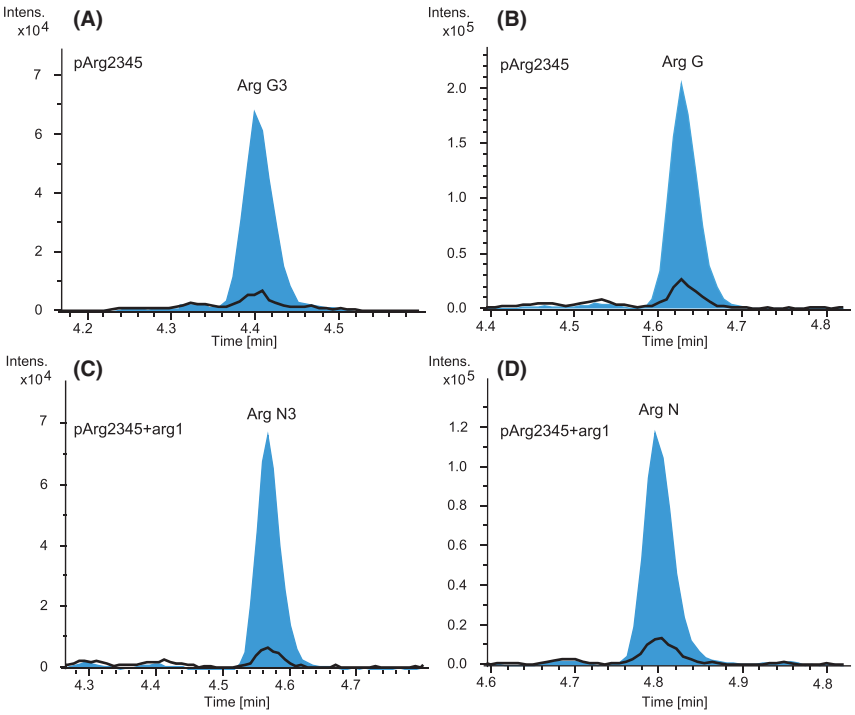

Fig. 7. EICs of argyrin G3 $[M + H]^+ = 825.313$ (A), argyrin G $[M + H]^+ = 855.324$ (B), argyrin N3 $[M + H]^+ = 839.329$ (C) and argyrin N $[M + H]^+ = 869.339$ (D) produced by cultivation in the medium supplemented with L-serine (black) and with D/L-serine (blue).

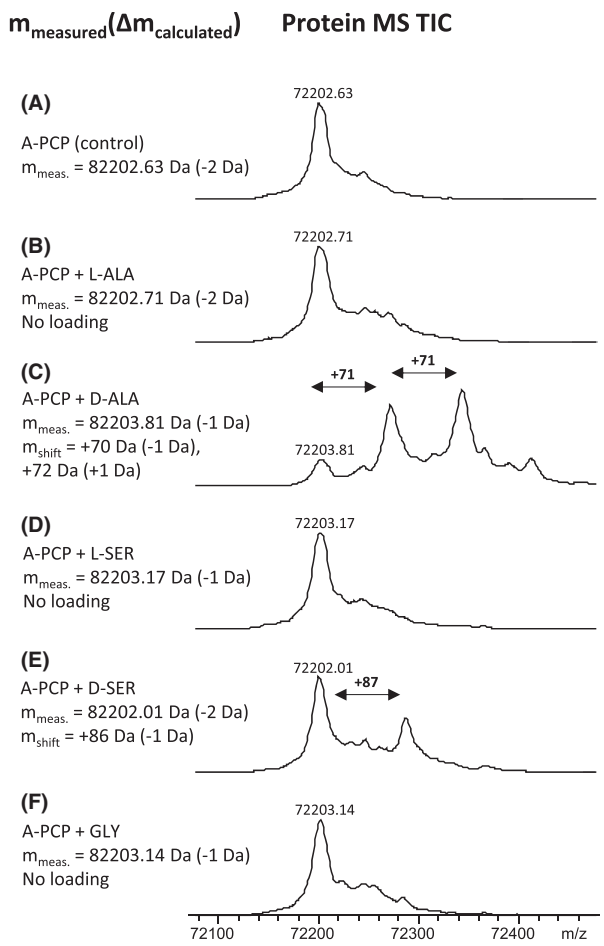

Fig. 8. Substrate specificity of the A4 domain of the argyrin NRPS. Observed mass shifts in deconvoluted protein MS TICs reveal loading of D-alanine (C) and D-serine (E), onto the PCP. L-alanine (B), L-serine (D) and glycine (F) were not accepted by A-PCP (control: A).

been observed in coumermycin (Schmutz *et al.*, 2003), novobiocic acid (Steffensky and Li, 2000), pacidamycin (Zhang *et al.*, 2011) and streptothricin (Maruyama *et al.*, 2012). In the latter case, the reaction is iterative and multiple incorporated building blocks can also be found in the final compound. This is not the case in argyrin and we can only assume that the C domain in the fourth module of the NRPS is selective for single PCP-bound amino acids or that the kinetics of the A domain is different *in vivo*. When the assay was performed with higher amino acid concentration (1mM), we have also observed triple loading of D-alanine, double loading of D-serine and glycine as well as single loading of L-alanine. The loading of L-serine could also not be observed in this case (Fig. S7). The generated data are consistent with results observed in the malachite green assay, confirming that the A domain is highly D-alanine and D-serine selective.

The results presented in this section indicate that the fourth module of the argyrin NRPS and the remaining downstream NRPS machinery favour incorporation and processing of D-serine over L-serine as long as the supply of D-serine is sufficient. A very limited production of D-serine-containing argyrin derivatives ($R_2 = CH_2OH$) in the absence of the external D-serine supply probably indicates a lack of a dedicated serine racemase in the genome of *M. xanthus*. This hypothesis was supported by a BLAST search in *M. xanthus*, using a serine racemase from *Roseobacter litoralis* Och 149 (Kubota *et al.*, 2016) as the template, which found no close serine racemase homologues. The question that arises here is where the small amount of D-serine originates from in case it is not externally added to the medium. We assume that after the depletion of D-serine only D-alanine is incorporated by the argyrin NRPS instead. Indeed, the supply of D-alanine could be ensured by an alanine racemase encoded in the genome of *M. xanthus* DK1622, which could be confirmed by a BLAST search (GenBank accession: SDW08429.1). Alanine racemases catalyse racemization between L- and D-alanine and are commonly found in bacteria as D-alanine is an essential component of the bacterial cell wall (Strych *et al.*, 2000; Liu *et al.*, 2018). However, various alanine or broad-spectrum racemases have also previously been shown to act promiscuously and catalyse L- to D-serine conversion (Esaki and Walsh, 1986; Asano and Endo, 1988). The trace amounts of D-serine-containing argyrin derivatives that can be detected even if the medium is not supplemented by D-serine could thus potentially originate from the medium components or from the activity of potential racemases with broad substrate spectrum present in the genome.

Conclusion

In this study we achieved conversion of argyrins A and B to their methylated counterparts, argyrins C and D, by reconstitution of the radical SAM-dependent methyltransferase Arg1. This is especially important as argyrins C and D recently showed improved immunomodulatory activity compared with the unmethylated argyrins A and B (Almeida *et al.*, 2021). Additionally, the cultivation conditions were adapted to allow exclusive production of specific argyrin derivatives by exploitation of the gatekeeper domain promiscuity in modules 1 and 4 of the argyrin NRPS. This broad substrate promiscuity of certain A and C domains should be studied further and could be employed in the future to, e.g. enable precursor-directed biosynthesis for production of more and novel argyrins. By supplementing the production medium with D-serine, we were able to shed light on the substrate preference of the fourth module of the argyrin

NRPS. This experiment simultaneously resulted in an improved production of D-serine-containing derivatives and also led to the identification of eight novel argyrin derivatives. Furthermore, we were able to show that the A domain from the fourth module of the argyrin NRPS is indeed highly selective for D-configured alanine and serine residues, by protein expression and *in vitro* characterization. In addition to increased production titres of argyrins A and B, improved production conditions in this work led to a substantial increase in the precursor product argyrin I, which could be converted into argyrin B or D by coexpression of additional *arg45* or *arg451* copies respectively. Notably, an expression of a single *arg1* gene copy in case of the *arg451* coexpression did not suffice to fully convert argyrin B to argyrin D. Therefore, an additional copy of *arg1* might be added in the future to resolve this bottleneck. Furthermore, the total production of argyrin was significantly improved by implementation and optimization of different promoter systems. The library of evaluated promoters provides a valuable source of information which will be useful in future studies with the aim to optimize the heterologous production of other secondary metabolites in *M. xanthus* DK1622. Overall, the herein presented improved argyrin production platform enables the production of single derivatives at nearly 400 mg l^{-1}. Since argyrins recently showed very promising potential as immunomodulators, this platform will certainly serve as a highly versatile tool to meet the supply–demand required for further preclinical testing and for production of novel argyrin derivatives in the future.

Experimental procedures

Construction and engineering of plasmids

Routine handling of nucleic acids, such as isolation of plasmid DNA, restriction endonuclease hydrolysis, DNA ligation and other DNA manipulations, was performed according to standard protocols (Sambrook and Russell, 2001). *E. coli* HS996 (Invitrogen, Waltham, MA, USA) was used as host for standard cloning experiments. *E. coli* strains were cultured in LB medium [1% tryptone, 0.5% yeast extract and 0.5% NaCl (1.5% agar)] at 30–37°C (and 200 rpm) overnight. Antibiotics were used as selection markers at the following final concentrations: 100 μg ml^{-1} ampicillin, 50 μg ml^{-1} kanamycin, 12 μg ml^{-1} tetracycline and 50 μg ml^{-1} zeocin. Transformation of *E. coli* strains was achieved *via* electroporation in 0.1-cm-wide cuvettes at 1250 V, a resistance of 200 Ω and a capacitance of 25 μF. Plasmid DNA was either purified by standard alkaline lysis (Sambrook and Russell, 2001), by using the GeneJet Plasmid Miniprep Kit (Thermo Fisher Scientific, Waltham, MA, USA), or the NucleoBond PC100 kit (Macherey Nagel, Düren, Germany). Restriction endonucleases, alkaline phosphatase (FastAP) and T4 DNA ligase were obtained from Thermo Fisher Scientific. Oligonucleotides used for PCR and Sanger sequencing were obtained from Sigma-Aldrich and are listed in Table S1. PCR reactions were carried out in a Mastercycler® pro (Eppendorf SE, Hamburg, Germany) using Phusion™ High-Fidelity, Taq DNA polymerase (Thermo Fisher Scientific) or Dream Taq DNA polymerase (Thermo Fisher Scientific) according to the manufacturer's protocol. For Taq and Dream Taq polymerase-based PCR experiments, the initial denaturation was 5 min at 95°C, followed by 30 cycles of denaturation (30 s, 95°C), annealing (30 s, 53–64°C), elongation (1 kb min^{-1}, 72°C) and final extension (10 min, 72°C). For Phusion™ polymerase-based PCR experiments, the initial denaturation was 2 min at 98°C, followed by 30 cycles of denaturation (20 s, 98°C), annealing (25 s, 53–64°C) and elongation (0.5 kb min^{-1}, 72°C); and final extension (10 min, 72°C). PCR products or DNA fragments from restriction hydrolysis were purified from agarose gel after agarose gel electrophoresis and isolated using the NucleoSpin® Gel and PCR Clean-up (Macherey-Nagel) or peqGold Gel Extraction (Peqlab). Red/ET recombineering experiments for plasmid modifications (Zhang *et al*., 1998) were performed according to the manufacturers' protocol (Gene Bridges GmbH, Heidelberg, Germany) using the strain *E. coli* GB05-red. After selection with suitable antibiotics, clones harbouring correct recombination products were identified by plasmid isolation followed by an independent hydrolysis with different endonucleases (leading to characteristic DNA band pattern in agarose-GE). Synthetic DNA fragments were obtained from ATG:biosynthetics GmbH and delivered in pGH-based standard cloning vectors (Table S2). Details on the construction of plasmids generated in this study are given in Table S3.

Construction of pUC18-zeo-Hom-arg1B expression construct

The primers dpo-pUC18-F and dpo-pUC18-R (Table S1) were used to amplify a 731 bp DNA fragment from pUC18, containing the origin of replication (ori), *via* PCR using Phusion polymerase. The respective PCR fragment was ligated with the chemically synthesized zeo-Hom-MCS fragment after restriction hydrolysis with PmeI and SpeI restriction endonucleases, generating the pUC18-zeo-Hom-MCS expression vector. The primers dpo-arg1F and dpo-arg1R (Table S1) were used to amplify a 238 bp *arg1* extension fragment from *Cystobacter* sp. SBCb004 genomic DNA *via* PCR using Phusion polymerase. Since no obvious ribosomal binding site (RBS) sequence could be identified upstream of the *arg1*, an RBS from *mchA* [AAGGAGG (Fu *et al*., 2008)]

was introduced *via* sequence extension of the forward primer (Table S1). The resulting PCR fragment was ligated into the pGH-arg1-V1 plasmid after restriction hydrolysis with NdeI and EcoRI, generating pGH-arg1B, harbouring the reconstituted *arg1* sequence. The pGH-arg1-V1 plasmid was obtained by gene synthesis and harbours a truncated version of the *arg1* gene without the 5' terminus. The 2047 bp *arg1* gene fragment was released from pGH-arg1B plasmid and inserted into previously constructed pUC18-zeo-Hom-MCS expression vector by ligation after restriction hydrolysis using NdeI and BglII, yielding the pUC18-zeo-Hom-arg1B expression construct (Table S3).

Construction of pUC18-Zeo-mx8-PnptII-arg45 and pUC18-Zeo-mx8-PnptII-arg451 expression constructs

The DNA fragments *arg1* (2054 bp) and *arg45* (2272 bp) were amplified by PCR using Phusion polymerase, pUC18-Zeo-Hom-arg1 and pArg2345-V1-BsaI plasmids as templates and dpo-arg1-2F/dpo-arg1-2R and dpo-arg4-5-F/dpo-arg4-5-R as primer pairs (Table S1) respectively. The *arg45* fragment was cloned into the pUC18-Zeo-Hom-arg1 plasmid *via* restriction hydrolysis with NdeI and NsiI and DNA ligation. The generated plasmid pUC18-Zeo-mx8-nptII-arg45 and the *arg1* PCR fragment were then hydrolysed with NsiI and BglII and ligated to yield the pUC18-Zeo-mx8-nptII-arg451 expression construct.

Design and construction of new synthetic promoter systems to replace the P_{ntpII} *promoter in the argyrin expression construct*

To evaluate the influence of other promoter systems on the production titre of argyrin, six new expression constructs with different promoter-5'-untranslated region (5'-UTR) combinations were designed. To minimize the transcriptional/translational influence of the native 5'-UTRs downstream of each promoter, a synthetically engineered 31-bp-long 5'-UTR (TACGAGAGCAAAAACGAGGAGAGGAGAAGAT) optimized for expression in *M. xanthus* DK1622 was designed using the RBS calculator tool (Salis and Mirsky, 2009; Espah Borujeni and Channarasappa, 2014), chemically synthesized and used to replace the native 5'-UTR region. Each synthetic fragment consisted of specific promoter followed by the 5'-UTR region and the first 61 bp of the downstream *arg2* gene and a unique StuI restriction endonuclease recognition sequence/site (R-site) at the 3' end. For cloning purposes, all constructs were also flanked by a *Swa*I R-site at the 5' end, allowing integration into the pArg2345-V1-BsaI expression construct as outlined in the Fig. S3. To design the nptII-synRBS-arg2 synthetic fragment, based on the P_{nptII} of the neomycin phosphotransferase II resistance gene from Tn5 (Beck *et al*., 1982), we used the same promoter sequence as originally used in the pArg2345-V1-BsaI expression construct. The only modification was the replacement of the 5'-UTR region with the new, synthetic one and the introduction of the flanking restriction sites for the cloning purposes. The sequence of P_{van} (Iniesta *et al*., 2012) was used to design the Pvan-synRBS-arg2 fragment and only the first 100 bp of the original P_{van} promoter sequence was implemented to design the Pvan-wo_vanR-synRBS-arg2 fragment with deleted repressor sequence in an attempt to make it function as a constitutive promoter system. The same approach was used in case of P_{tet} system (Chai *et al*., 2012), to design Ptet-synRBS-arg2 and Ptet-wo_tetR-synRBS-arg2 constructs. The first 63 bp of the *tet* promoter sequence was used for the promoter version lacking the associated repressor gene. In case of the P_{pm}, originating from *Pseudomonas putida*, the improved version of the promoter system, generated by random mutagenesis approach (Bakke *et al*., 2009), was used to design the Ppm-synRBS-arg2 sequence. For assembly purposes, the *Stu*I R-site present in the promoter sequence had to be removed by exchange of a single nucleotide. The P_{pm} normally acts as an inducible promoter in pseudomonads; however, in *M. xanthus,* it was shown to work constitutively (Perlova *et al*., 2006). The promoter fragments with the lengths of 233 bp (P_{pm}), 803 bp (P_{tet}), 169 bp ($P_{tet\Delta R}$), 245 bp (P_{nptII}), 1145 bp (P_{van}) and 200 bp ($P_{van\Delta R}$) were released from the respective gene synthesis vectors and ligated into the pArg2345-V1-BsaI expression vector after restriction hydrolysis with SwaI and StuI.

Transformation and chromosomal integration of expression constructs into M. xanthus *DK1622*

According to a previously established electroporation procedure for *M. xanthus* DK1622 (Kashefi and Hartzell, 1995), the host strain *Mx*. DK1622::pArg2345 (Pogorevc *et al*., 2019b) was transformed with the generated expression construct pUC18-zeo-Hom-arg1B (Table S3). *M. xanthus* DK1622 mutants were cultivated at 30°C in CTT medium [1% casitone, 10 mM Tris buffer pH 7.6, 1 mM KH_2PO_4 pH 7.6 and 8 mM $MgSO_4$ (1.5% agar) with final pH 7.6]. For liquid cultures, the strains were grown in Erlenmeyer flasks on an orbital shaker at 180 rpm for 2–3 days. For selection of *M. xanthus* mutants, 50 $\mu g\ ml^{-1}$ kanamycin and 50 $\mu g\ ml^{-1}$ zeocin were used. After electroporation, the transformed cells were re-suspended in 1 ml CTT medium and incubated for 6 h under constant shaking. Afterward, the transformants were mixed with 3 ml of CTT soft agar (CTT with only 7.5 $g\ l^{-1}$ agar) and poured onto a CTT agar plate.

After hardening of the soft agar layer with embedded transformant cells, the plates were incubated at 30°C for 5 days. Embedding in the soft agar prevented swarming of the transformant colonies over the agar surface, allowing the isolation of single clones and transfer onto a fresh CTT agar plate. Correct chromosomal integration of the *arg1* expression construct into the downstream locus of the previously integrated argyrin BGC (Pogorevc *et al*., 2019b) or the argyrin BGC expression constructs into the *tetR* locus of the *M. xanthus* DK1622*ΔmchA-tet* mutant *via* homologous recombination was verified by PCR (Fig. S1). Transformant cells (1 cm^2) were scratched from the plate, re-suspended in 50 μl of water and subsequently lysed by incubating at 95°C for 30 min prior of being added to the PCR reaction ('colony PCR'). For each expression construct, correct chromosomal integration was confirmed using two primer combinations, revealing PCR products of the expected sizes: P5/P6 (1261 bp) and P7/P8 (1401 bp) for the *arg1* expression construct and P1/P2 (1458 bp) and P3/P4 (1461 bp) for argyrin BGC expression constructs. Genomic DNA of *Mx*. DK1622::pArg2345 or *M. xanthus* DK1622*ΔmchA-tet* isolated using Qiagen Puregene Core Kit A was used as negative control. The complementary experiment using primers P5/P8 or P1/P4 revealed a 1112 bp PCR products for *Mx*. DK1622::pArg2345 or a 1461 bp PCR product for *M. xanthus* DK1622*ΔmchA-tet* respectively. The same primer pairs yielded no PCR product in the expression strains.

Correct chromosomal integration of plasmids integrated by the mx8 integrase was performed using two primer combinations, revealing PCR products of the expected sizes: P9/P10 (403 bp) and P11/P12 (427 bp). Genomic DNA of *Mx*. DK1622::pArg2345 was used as negative control. The complementary experiment using primers P9/P12 revealed a 449 bp PCR product for *Mx*. DK1622::pArg2345, but not for the expression strains (Fig. S2). PCR reactions were performed according to the above described conditions, using Taq polymerase; for primer sequences, see Table S1.

Cultivation conditions of argyrin producer strains

To vary the production between different argyrin derivatives (e.g. argyrins A, B, C and D), strains *Mx*. DK1622::pArg2345 and *Mx*. DK1622::pArg2345-arg1 were cultivated in CTT and M7/s4 medium (0.5% soy flour, 0.5% corn starch, 0.2% glucose, 0.1% yeast extract, 0.1% $MgSO_4$ x 7 H_2O, 0.1% $CaCl_2$ x 2 H_2O, 1% HEPES, with final pH 7.4 and supplemented with 0.1 mg l^{-1} of vitamin B12 and 5 mg l^{-1} of $FeCl_3$ after autoclaving) with and without supplementation of 10 mM L-Abu. To evaluate the effect of different expression constructs on the argyrin production profile, the heterologous producers with replaced promoter were used for parallel cultivation in the M7/s4 production medium supplemented with amino acids, calculated to the final concentration of 5 mM L-serine, 5 mM L-cysteine, 5 mM L-alanine, 10 mM L-tryptophan, 10 mM glycine and 10 mM L-Abu, before autoclaving. In case of inducible promoters (P_{tet} or P_{van}), the respective cultures were supplemented with 0.7 μg ml^{-1} tetracycline or 1 mM vanillate respectively. To verify if D-alanine is directly activated by the argyrin NRPS, argyrin producer strains *Mx*. DK1622::pArg2345, *Mx*. DK1622::pArg2345-arg45, *Mx*. DK1622::pArg2345-arg1 and *Mx*. DK1622::pArg2345-arg451 were cultivated in the M7/s4 medium supplemented with 5 mM L-serine or D/L-serine in addition to other argyrin substrate amino acids mentioned above. Furthermore, *Mx*. DK1622::pArg2345-arg1 was also cultivated in M7/s4 medium supplemented with argyrin substrate amino acids (as described for the promoter screening experiment) and D/L-serine without the addition of L-Abu. Strains were inoculated from cryo stocks and grown on CTT agar plates supplemented with kanamycin 50 μg ml^{-1} (*Mx*. DK1622::pArg2345) or with kanamycin 50 μg ml^{-1} and zeocin 50 μg ml^{-1} (*Mx*. DK1622::pArg2345-arg1) for several days until the plates were mostly overgrown with swarming cells. All of the cells were scraped from the plates to inoculate M7/s4 preculture medium (50 ml medium in 300 ml Erlenmeyer flask) and the seed cultures were cultivated at 30°C, 180 rpm on an orbital shaker (Infors HT) for 48 h. Five millilitre of the preculture was used to inoculate 50 ml of the M7/s4 production medium in which the strain was grown under the same conditions for 6 days. All cultures were supplemented with suitable antibiotics as mentioned above and production cultures were additionally supplemented with 4% Amberlite XAD-16 resin. All strains were initially cultivated in biological triplicates and technical triplicates of one clone were cultivated in the follow-up experiments. The cultivations took 6–8 days before harvesting by centrifugation at 8000 rpm for 15 min, and after the supernatant was removed the pelleted cells with Amberlite XAD-16 resin were extracted with 50 ml of ethyl acetate twice. The extracts were filtered and dried in round bottom flasks on a rotary evaporator. The crude extracts were dissolved in 1 ml of methanol and subjected to HPLC-MS analysis.

Analysis of the argyrin production by HPLC-MS

Argyrin samples were routinely analysed on a Dionex Ultimate 3000 RSLC system using a Waters BEH C_{18} column (50 × 2.1 mm, 1.7 μm) equipped with a Waters VanGuard BEH C_{18} 1.7 μm guard column. Separation of 1 μl sample (crude extract 1/5 dilutions in methanol) was achieved by a linear gradient from (A) H_2O + 0.1% FA to

(B) ACN + 0.1% FA at a flow rate of 600 μl min^{-1} and a column temperature of 45°C. Gradient conditions were as follows: 0–0.5 min, 5% B; 0.5–18.5 min, 5–95% B; 18.5–20.5 min, 95% B; 20.5–21 min, 95–5% B; and 21–22.5 min, 5% B. UV spectra were recorded by a DAD in the range from 200 to 600 nm. The LC flow was split to 75 μl min^{-1} before entering the Bruker Daltonics maXis 4G hr-qToF mass spectrometer using the Apollo II ESI source. Mass spectra were acquired in centroid mode ranging from 150 to 2500 m/z at a 2 Hz full scan rate. Mass spectrometry source parameters were set to 500 V as end plate offset; 4000 V as capillary voltage; nebulizer gas pressure 1 bar; dry gas flow of 5 l min^{-1} and a dry temperature of 200°C. Ion transfer and quadrupole settings were set to Funnel RF 350 Vpp; Multipole RF 400 Vpp as transfer settings and ion energy of 5 eV as well as a low mass cut of 300 m/z as Quadrupole settings. Collision cell was set to 5.0 eV and pre pulse storage time was set to 5 μs. Spectra acquisition rate was set to 2 Hz. Calibration of the maXis4G qTOF spectrometer was achieved with sodium formate clusters before every injection to avoid mass drifts. All MS analyses were acquired in the presence of the lock masses $C_{12}H_{19}F_{12}N_3O_6P_3$, $C_{18}H_{19}O_6N_3P_3F_2$ and $C_{24}H_{19}F_{36}N_3O_6P_3$ which generate the $[M + H]^+$ ions of 622.028960, 922.009798 and 1221.990638. The corresponding MS^2 method operating in automatic precursor selection mode picks up the two most intense precursors per cycle, applies smart exclusion after five spectra and performs CID and MS/MS spectra acquisition time ramping. CID energy was ramped from 35 eV for 500 m/z to 45 eV for 1000 m/z and 60 eV for 2000 m/z. MS full scan acquisition rate was set to 2 Hz, and MS/MS spectra acquisition rates were ramped from 1 to 4 Hz for precursor Ion intensities of 10 kcts to 1000 kcts.

To quantify argyrin production levels, the following HPLC-MS method was applied. Separation was performed on a Dionex UltiMate 3000 RSLC system equipped with a Waters reversed phase UPLC column (Acquity UPLC BEH C18 1.7 μm; 2.1 × 100 mm) using a linear gradient with solvent A (water + 0.1% formic acid) and B (acetonitrile + 0.1% formic acid) at a flow rate of 600 μl min^{-1} and 45°C. The gradient was initiated by a 0.5 min isocratic step with 5% B followed by an increase to 15% B within 1 min, 50% B within 11.5 min and 95% B within 1 min, which was kept for 1 min, before decreasing back to initial conditions of 5% B within 0.3 min and was kept for 1.7 min. HPLC was coupled to a Bruker Daltonics ion trap mass spec 'Amazon speed' system. Mass spectra were acquired in positive ionization mode with a range 200–2500 m/z at a resolution of R = 30000. Identities of the argyrins were confirmed by comparing both retention time and MS^2 fragmentation pattern with authentic standards.

Quantification was performed using Bruker Daltonics Quant analysis software version 4.4. The following method was used to quantify the corresponding derivatives; argyrin I (retention time 9.83 min, MS^2 fragments: 707.2; 724.2), argyrin A (retention time 10.05 min, MS^2 fragments: 737.3; 754.3), argyrin B (retention time 10.60, MS^2 fragments: 737.3; 754.3), argyrin C (retention time 10.71 min, MS^2 fragments: 751.3; 768.3) and argyrin D (retention time 11.28 min, MS^2 fragments: 751.3; 768.3).

Expression and purification of A-PCP bidomain

To express the A-PCP bidomain from the fourth module of the argyrin NRPS (*arg3* nucleotide 1306-3262), the respective 2014-bp-long DNA fragment was amplified by PCR from the pArg2345-V1-BsaI expression plasmid using the primer pair dpo-A-PCP-TEV-BamHI-F2/dpo-A-PCP-HindIII-R (Table S1). The product was hydrolysed using BamHI/HindIII and ligated into similarly digested pETDuet™-1_MXAN_3118 expression vector (unpublished data), which already contained a gene-encoding MbtH-like protein homologue from *M. xanthus* (NCBI locus tag: MXAN_RS15115), to be coexpressed [without the histidine (his) tag] together with the A-PCP protein. The resulting pETDuet™-1_MXAN_3118-argM4-A-PCP plasmid was transformed into an *E. coli* BL21 (DE3) for protein expression and a single colony was picked to inoculate 100 ml LB broth containing 100 mg ml^{-1} ampicillin, which was incubated at 37°C overnight with shaking at 200 rpm. The overnight culture was used to inoculate 6 litres of fresh LB medium containing 100 mg ml^{-1} ampicillin. After growing at 37°C until OD_{600} of 0.5–0.6, the expression of the A-PCP was induced by addition of 0.4 mM IPTG. The culture was further incubated at 16°C for 24 h. The next day, the cells were pelleted by centrifugation at 8000 rpm. Cell pellets were re-suspended in 80 ml of the lysis buffer (20 mM TrisHCl pH 8, 500 mM NaCl, 0.1% triton X-100 (V/V), 20 mM imidazole, 1 mM DTT) and lysed using a cell disruptor (Constant systems) at 30.000 psi. The cell lysate was centrifuged at 20 000 rpm for 20 min at 4°C. The supernatant was filtered using the MF-Millipore 0.45 μm filter and afterwards loaded onto a pre-equilibrated (lysis buffer) 5 ml Histrap HP column (GE healthcare, Chicago, IL, USA) and was washed with 20 column volumes of lysis buffer. The bound his-tagged A-PCP protein was eluted with 5 column volumes of buffer containing 250 mM imidazole. The eluent was injected onto a desalting column (Desalt 16/10, GE healthcare) and the chromatography was conducted using the buffer without imidazole or detergent [20 mM TrisHCl pH 8, 200 mM NaCl and 1 mM tris(2-carboxyethyl)phosphine (TCEP)] at a flow rate of 10 ml min^{-1}. The protein in the fractions was monitored by UV absorbance at 280 nm

and the protein containing fractions were pooled. The protein containing eluate was digested with a tobacco etch virus (TEV) protease in a mass-to-mass ratio of 1:10 overnight at 4°C to cleave the his tag. Digested protein was then passed over a second Histrap HP column, and the flow through was collected and concentrated to around 7 ml using an Amicon Ultracel-50 centrifugal filter unit with a molecular weight cut-off of 50 kDa. The concentrated protein was loaded onto a gel filtration column (HiLoad 16/600 Superdex 200 pg, GE healthcare) pre-equilibrated with the gel filtration buffer (20 mM TrisHCl pH 8, 200 mM NaCl and 1 mM TCEP). The fractions of the highest purity were pooled together and concentrated to 5 mg ml^{-1}. The identity of the protein was confirmed using protein MS.

Malachite green assay

Characterization of the adenylation domain specificity was performed by malachite green colorimetric assay as previously described (McQuade *et al*., 2009). The reaction mixture contained 1.6 μl of 1 M Tris-HCl buffer (pH 8); 3.2 μl of 5 M NaCl, 8 μl of 100 mM $MgCl_2$; 0.5 μl of pyrophosphatase; 3.2 μl of 10 μM expressed protein (A-PCP); 0.2 μl of 100 mM ATP and 60.9 μl of H_2O. The reaction was finally started by addition of 2.4 μl of 25 mM amino acid solution. We have tested the reaction with L- and D-alanine, L- and D-serine and glycine. All reactions were prepared in triplicates in a 96 well plate and incubated either 1 h at 30°C or overnight at room temperature with shaking at 300 rpm. After the incubation, 20 μl of malachite green phosphate assay kit reagent a and b mixture (100 : 1) from Sigma-Aldrich was added and the absorbance was measured at 620 nm with a TECAN Infinite® M Nano plate reader directly and again after 30 min.

Protein loading assay

The protein loading assay was performed by preparing a reaction mixture containing 10 μM expressed protein (A-PCP), 10 mM $MgCl_2$, 2 mM ATP, 20 mM Tris-HCl (pH 8), 200 mM NaCl and 1 mM, 100 μM, 10 μM or 1 μM amino acid solution (L- or D-alanine, L- or D-serine or glycine). The mixture was incubated overnight at room temperature with shaking at 300 rpm before the samples were subjected to HPLC-MS analysis.

Analysis of the in vitro protein reactions by HPLC-MS

All ESI-MS measurements were performed on a Dionex Ultimate 3000 RSLC system using an Aeris Widepore XB-C8, 150 x 2.1 mm, 3.6 μm dp column (Phenomenex, Torrance, CA, USA). Separation of 2 μl sample was achieved by a linear gradient from (A) H2O + 0.1% FA to (B) ACN + 0.1% FA at a flow rate of 300 μl min^{-1} and 45°C. The gradient was initiated by a 1.0 min isocratic step at 2% B, followed by an increase to 75% B in 10 min to end up with a 3 min step at 75% B before re-equilibration with initial conditions. UV spectra were recorded by a DAD in the range from 200 to 600 nm. The LC flow was split to 75 μl min^{-1} before entering the maXis 4G hr-ToF mass spectrometer (Bruker Daltonics, Bremen, Germany) using the standard Bruker ESI source. In the source region, the temperature was set to 200°C, the capillary voltage was 4000 V, the dry-gas flow was 5.0 l min^{-1} and the nebulizer was set to 1.0 bar. Mass spectra were acquired in positive ionization mode ranging from 150 to 2500 m/z at 2 Hz scan rate. Protein masses were deconvoluted by using the Maximum Entropy algorithm (Copyright 1991-2004 Spectrum Square Associates).

Acknowledgements

This work was supported by DZIF. We would like to thank Daniel Sauer, Sophia Panter and Matej Rebek for excellent technical assistance. We would also like to thank Dr. Asfandyar Sikandar and Jan Dastbaz for excellent assistance and advice regarding protein expression and *in vitro* assays as well as Jan Dastbaz for providing the pETDuet™-1_MXAN_3118 plasmid. Finally, we would like to thank Dr. Sebastian Groß for proofreading this manuscript.

Conflict of interest

None declared.

Data Availability Statement

The sequences of the expression constructs have been deposited in the GenBank database under the following accession numbers: MZ634479-MZ634488.

References

Allardyce, D.J., Bell, C.M., and Loizidou, E.Z. (2019) Argyrin B, a non-competitive inhibitor of the human immunoproteasome exhibiting preference for β1i. *Chem Biol Drug Des* **94:** 1556–1567.

Almeida, L., Dhillon-LaBrooy, A., Castro, C.N., Adossa, N., Carriche, G.M., Guderian, M., *et al*. (2021) Ribosome-targeting antibiotics impair T cell effector function and ameliorate autoimmunity by blocking mitochondrial protein synthesis. *Immunity* **54:** 68–83.e6.

Altschul, S.F., Gish, W., Miller, W., Myers, E.W., and Lipman, D.J. (1990) Basic local alignment search tool. *J Mol Biol* **215:** 403–410.

Asano, Y., and Endo, K. (1988) Amino acid racemase with broad substrate specificity, its properties and use in phenylalanine racemization. *Appl Microbiol Biotechnol* **29:** 523–527.

Bakke, I., Berg, L., Aune, T.E., Brautaset, T., Sletta, H., Tondervik, A., and Valla, S. (2009) Random mutagenesis of the Pm promoter as a powerful strategy for improvement of recombinant gene expression. *Appl Environ Microbiol* **75:** 2002–2011.

Beck, E., Ludwig, G., Auerswald, E.A., Reiss, B., and Schaller, H. (1982) Nucleotide sequence and exact localization of the neomycin phosphotransferase gene from transposon Tn5. *Gene* **19:** 327–336.

Bülow, L., Nickeleit, I., Girbig, A.-K., Brodmann, T., Rentsch, A., Eggert, U., *et al*. (2010) Synthesis and biological characterization of argyrin F. *ChemMedChem* **5:** 832–836.

Canafax, D.M., and Ascher, N.L. (1983) Cyclosporine immunosuppression. *Clin Pharm* **2:** 515–524.

Chai, Y., Shan, S., Weissman, K.J., Hu, S., Zhang, Y., and Müller, R. (2012) Heterologous expression and genetic engineering of the tubulysin biosynthetic gene cluster using Red/ET recombineering and inactivation mutagenesis. *Chem Biol* **10:** 361–371.

Chen, C.H., Genapathy, S., Fischer, P.M., and Chan, W.C. (2014) A facile approach to tryptophan derivatives for the total synthesis of argyrin analogues. *Org Biomol Chem* **12:** 9764–9768.

Dumont, F.J., and Su, Q. (1995) Mechanism of action of the immunosuppressant rapamycin. *Life Sci* **58:** 373–395.

Dvir, S., Velten, L., Sharon, E., Zeevi, D., Carey, L.B., Weinberger, A., and Segal, E. (2013) Deciphering the rules by which 5'-UTR sequences affect protein expression in yeast. *Proc Natl Acad Sci USA* **110:** E2792–E2801.

Esaki, N., and Walsh, C.T. (1986) Biosynthetic alanine racemase of *Salmonella typhimurium*: purification and characterization of the enzyme encoded by the alr gene. *Biochemistry* **25:** 3261–3267.

Espah Borujeni, A., Channarasappa, A.S., and Salis, H.M. (2014) Translation rate is controlled by coupled trade-offs between site accessibility, selective RNA unfolding and sliding at upstream standby sites. *Nucleic Acids Res* **42:** 2646–2659.

Finking, R., and Marahiel, M.A. (2004) Biosynthesis of nonribosomal peptides. *Annu Rev Microbiol* **58:** 453–488.

Fu, J., Wenzel, S.C., Perlova, O., Wang, J., Gross, F., Tang, Z., *et al*. (2008) Efficient transfer of two large secondary metabolite pathway gene clusters into heterologous hosts by transposition. *Nucleic Acids Res* **36:** e113.

Gemperlein, K., Rachid, S., Garcia, R.O., Wenzel, S.C., and Müller, R. (2014) Polyunsaturated fatty acid biosynthesis in myxobacteria. Different PUFA synthases and their product diversity. *Chem Sci* **5:** 1733–1741.

Groß, S., Schnell, B., Haack, P.A., Auerbach, D., and Müller, R. (2021) In vivo and in vitro reconstitution of unique key steps in cystobactamid antibiotic biosynthesis. *Nat Commun* **12:** 1696.

Hug, J.J., Panter, F., Krug, D., and Müller, R. (2019) Genome mining reveals uncommon alkylpyrones as type III PKS products from myxobacteria. *J Ind Microbiol Biotechnol* **46:** 319–334.

Iniesta, A.A., García-Heras, F., Abellón-Ruiz, J., Gallego-García, A., and Elías-Arnanz, M. (2012) Two systems for conditional gene expression in *Myxococcus xanthus* inducible by isopropyl-ß-D-thiogalactopyranoside or vanillate. *J Bacteriol* **194:** 5875–5885.

Ishikawa, J., and Hotta, K. (1999) FramePlot: a new implementation of the frame analysis for predicting protein-coding regions in bacterial DNA with a high G + C content. *FEMS Microbiol Lett* **174:** 251–253.

Julien, B., and Shah, S. (2002) Heterologous expression of epothilone biosynthetic genes in *Myxococcus xanthus*. *Antimicrob Agents Chemother* **46:** 2772–2778.

Kaniusaite, M., Tailhades, J., Kittilä, T., Fage, C.D., Goode, R.J.A., Schittenhelm, R.B., and Cryle, M.J. (2021) Understanding the early stages of peptide formation during the biosynthesis of teicoplanin and related glycopeptide antibiotics. *FEBS J* **288(2):** 507–529.

Kano, S., Suzuki, S., Hara, R., and Kino, K. (2019) Synthesis of d-amino acid-containing dipeptides using the adenylation domains of nonribosomal peptide synthetase. *Appl Environ Microbiol* **85:** e00120-19.

Kashefi, K., and Hartzell, P.L. (1995) Genetic suppression and phenotypic masking of a *Myxococcus xanthus* frzF- defect. *Mol Microbiol* **15:** 483–494.

Kim, H.J., McCarty, R.M., Ogasawara, Y., Liu, Y.-N., Mansoorabadi, S.O., LeVieux, J., and Liu, H. (2013) GenK-catalyzed C-6' methylation in the biosynthesis of gentamicin: Isolation and characterization of a cobalamin-dependent radical SAM enzyme. *J Am Chem Soc* **135:** 8093–8096.

Kubota, T., Shimamura, S., Kobayashi, T., Nunoura, T., and Deguchi, S. (2016) Distribution of eukaryotic serine racemases in the bacterial domain and characterization of a representative protein in *Roseobacter litoralis* Och 149. *Microbiology (Reading Engl)* **162:** 53–61.

Lau, J., Frykman, S., Regentin, R., Ou, S., Tsuruta, H., and Licari, P. (2002) Optimizing the heterologous production of epothilone D in *Myxococcus xanthus*. *Bioeng* **78:** 280–288.

Ley, S.V., Priour, A., and Heusser, C. (2002) Total synthesis of the cyclic heptapeptide argyrin B: a new potent inhibitor of T-cell independent antibody formation. *Org Lett* **4:** 711–714.

Liu, S., Wei, Y., Zhou, X., Zhang, K., Peng, X., Ren, B., *et al*. (2018) Function of alanine racemase in the physiological activity and cariogenicity of *Streptococcus mutans*. *Sci Rep* **8:** 5984.

Mann, J. (2001) Natural products as immunosuppressive agents. *Nat Prod Rep* **18:** 417–430.

Marahiel, M.A., Stachelhaus, T., and Mootz, H.D. (1997) Modular peptide synthetases involved in nonribosomal peptide synthesis. *Chem Rev* **97:** 2651–2674.

Maruyama, C., Toyoda, J., Kato, Y., Izumikawa, M., Takagi, M., Shin-ya, K., *et al*. (2012) A stand-alone adenylation domain forms amide bonds in streptothricin biosynthesis. *Nat Chem Biol* **8:** 791–797.

McQuade, T.J., Shallop, A.D., Sheoran, A., Delproposto, J.E., Tsodikov, O.V., and Garneau-Tsodikova, S. (2009) A nonradioactive high-throughput assay for screening and characterization of adenylation domains for nonribosomal peptide combinatorial biosynthesis. *Anal Biochem* **386:** 244–250.

Nickeleit, I., Zender, S., Sasse, F., Geffers, R., Brandes, G., Sörensen, I., *et al*. (2008) Argyrin A reveals a critical role for the tumor suppressor protein p27kip1 in mediating antitumor activities in response to proteasome inhibition. *Cancer Res* **14:** 23–35.

Oßwald, C., Zipf, G., Schmidt, G., Maier, J., Bernauer, H. S., Müller, R., and Wenzel, S. (2014) Modular construction of a functional artificial epothilone polyketide pathway. *ACS Synth Biol* **3:** 759–772.

Ongley, S., Bian, X., Neilan, B.A., and Müller, R. (2013) Recent advances in the heterologous expression of microbial natural product biosynthetic pathways. *Nat Prod Rep* **30:** 1121–1138.

Panter, F., Krug, D., Baumann, S., and Müller, R. (2018) Self-resistance guided genome mining uncovers new topoisomerase inhibitors from myxobacteria. *Chem Sci* **9:** 4898–4908.

Perlova, O., Fu, J., Kuhlmann, S., Krug, D., Stewart, F., Zhang, Y., and Müller, R. (2006) Reconstitution of myxothiazol biosynthetic gene cluster by Red/ET recombination and heterologous expression in *Myxococcus xanthus*. *Appl Environ Microbiol* **72:** 7485–7494.

Pierre, S., Guillot, A., Benjdia, A., Sandstrom, C., Langella, P., and Berteau, O. (2012) Thiostrepton tryptophan methyltransferase expands the chemistry of radical SAM enzymes. *Nat Chem Biol* **8:** 957–959.

Pogorevc, D., Panter, F., Schillinger, C., Jansen, R., Wenzel, S.C., and Müller, R. (2019a) Production optimization and biosynthesis revision of corallopyronin A, a potent anti-filarial antibiotic. *Metab Eng* **55:** 201–211.

Pogorevc, D., Tang, Y., Hoffmann, M., Zipf, G., Bernauer, H.S., Popoff, A., *et al*. (2019b) Biosynthesis and Heterologous Production of Argyrins. *ACS Synth. Biol* **8:** 1121–1133.

Rausch, C., Hoof, I., Weber, T., Wohlleben, W., and Huson, D.H. (2007) Phylogenetic analysis of condensation domains in NRPS sheds light on their functional evolution. *BMC Evol Biol* **7:** 78–92.

Salis, H.M., Mirsky, E.A., and Voigt, C.A. (2009) Automated design of synthetic ribosome binding sites to control protein expression. *Nat Biotechnol* **27:** 946–950.

Sambrook, J., and Russell, D.W. (2001) *Molecular Cloning: A Laboratory Manual*. Cold Spring Harbor, NY: Cold Spring Harbor Laboratory Press.

Schmutz, E., Steffensky, M., Schmidt, J., Porzel, A., Li, S.M., and Heide, L. (2003) An unusual amide synthetase (CouL) from the coumermycin A1 biosynthetic gene cluster from *Streptomyces rishiriensis* DSM 40489. *Eur J Biochem* **270:** 4413–4419.

Shi, G., Shi, N., Li, Y., Chen, W., Deng, J., Liu, C., *et al*. (2016) d-alanylation in the assembly of ansatrienin side chain is catalyzed by a m odular NRPS. *ACS Chem Biol* **11:** 876–881.

Stauch, B., Simon, B., Basile, T., Schneider, G., Malek, N.P., Kalesse, M., and Carlomagno, T. (2010) Elucidation of the structure and intermolecular interactions of a reversible cyclic-peptide inhibitor of the proteasome by NMR spectroscopy and molecular modeling. *Angew Chem Int Ed* **49:** 3934–3938.

Steffensky, M., Li, S.M., and Heide, L. (2000) Cloning, overexpression, and purification of novobiocic acid synthetase from *Streptomyces spheroides* NCIMB 11891. *J Biol Chem* **275:** 21754–21760.

Stevens, D.C., Henry, M.R., Murphy, K.A., and Boddy, C. N. (2010) Heterologous expression of the oxytetracycline biosynthetic pathway in *Myxococcus xanthus*. *Appl Environ Microbiol* **76:** 2861–2863.

Strych, U., Huang, H.C., Krause, K.L., and Benedik, M.J. (2000) Characterization of the alanine racemases from *Pseudomonas aeruginosa* PAO1. *Curr Microbiol* **41:** 290–294.

Sucipto, H., Pogorevc, D., Luxenburger, E., Wenzel, S. C., and Müller, R. (2017) Heterologous production of myxobacterial α-pyrone antibiotics in *Myxococcus xanthus*. *Metab Eng* **44:** 160–170.

Sun, Y., Feng, Z., Tomura, T., Suzuki, A., Miyano, S., Tsuge, T., *et al*. (2016) Heterologous production of the marine myxobacterial antibiotic haliangicin and its unnatural analogues generated by engineering of the biochemical pathway. *Sci Rep* **6:** 22091.

Süssmuth, R.D., and Mainz, A. (2017) Nonribosomal peptide synthesis - Principles and prospects. *Angew Chem Int Ed* **56:** 3770–3821.

Tu, Q., Herrmann, J., Hu, S., Raju, R., Bian, X., Zhang, Y., and Müller, R. (2016) Genetic engineering and heterologous expression of the disorazol biosynthetic gene cluster via Red/ET recombineering. *Sci Rep* **6:** 21066.

Wallemacq, P.E., and Reding, R. (1993) FK506 (tacrolimus), a novel immunosuppressant in organ transplantation: clinical, biomedical, and analytical aspects. *Clin Chem* **39:** 2219–2228.

Wenzel, S.C., Hoffmann, H., Zhang, J., Debussche, L., Haag-Richter, S., Kurz, M., *et al*. (2015) Production of the bengamide class of marine natural products in myxobacteria: biosynthesis and structure-activity relationships. *Angew Chem Int Ed Engl* **54:** 15560–15564.

Wu, T.S., Duncan, J., Tsao, S.W., Chang, C.J., Keller, P.J., and Floss, H.G. (1987) Biosynthesis of the ansamycin antibiotic ansatrienin (mycotrienin) by *Streptomyces collinus*. *J Nat Prod* **50:** 108–118.

Yan, F., Auerbach, D., Chai, Y., Keller, L., Tu, Q., and Hüttel, S. (2018a) Biosynthesis and heterologous production of vioprolides: Rational biosynthetic engineering and unprecedented 4-methylazetidinecarboxylic acid formation. *Angew Chem Int Ed Engl* **57:** 8754–8759.

Yan, F., Burgard, C., Popoff, A., Zaburannyi, N., Zipf, G., Maier, J., *et al*. (2018b) Synthetic biology approaches and combinatorial biosynthesis towards heterologous lipopeptide production. *Chem Sci* **9:** 7510–7519.

Zhang, Y., Buchholz, F., Muyrers, J.P.P., and StewartA, A.F. (1998) A new logic for DNA engineering using recombination in *E. coli*. *Nat Genet* **20:** 123–128.

Zhang, Q., van der Donk, W.A., and Liu, W. (2012) Radical-mediated enzymatic methylation: a tale of two SAMS. *Acc Chem Res* **45:** 555–564.

Zhang, W., Ntai, I., Bolla, M.L., Malcolmson, S.J., Kahne, D., Kelleher, N.L., and Walsh, C.T. (2011) Nine enzymes are required for assembly of the pacidamycin group of peptidyl nucleoside antibiotics. *Adv Ceram Mater* **133:** 5240–5243.

Supporting information

Additional supporting information may be found online in the Supporting Information section at the end of the article.

Fig. S1. Genotypic verification of integration of all argyrin cluster versions into the heterologous host *M. xanthus* DK1622 *ΔmchA-tet*. Primer sets used for genotypic verification, their binding sites and amplicon sizes are illustrated. Nucleotide sequences of the primers used are listed in the Table S1. Mch stands for myxochromide.

Fig. S2. Genotypic verification of insert integration into the mx8 attb1 site of the *Mx*. DK1622::pArg2345. Primer sets used for genotypic verification, their binding sites and amplicon sizes are illustrated. Nucleotide sequences of the primers used are listed in the Table S1.

Fig. S3. Assembly strategy for the exchange of the promoter systems upstream of the arg2345 operon. The same strategy was applied in case of all promoter fragments. The figure shows P_{tet} sequence as an example.

Fig. S4. Base peak chromatograms (BPCs) of the *Mx*. DK1622::pArg2345-arg451 MeoH (blue) and DMSO (black) crude extracts.

Fig. S5. Clustal Omega alignment of *Pseusomonas aeruginosa* PAO1 and *M. xanthus* DK1622 FusA1 sequences. The difference S459R (numbering according to the sequence of *P. aeruginosa* FusA1) is highlighted with an arrow.

Fig. S6. Visualization of argyrin B and the residue S459 of the *P. aeruginosa* FusA1 protein binding pocket (left). If the same residue is exchanged with R459 found in the *M. xanthus* DK1622 FusA1 sequence, this introduces a significant clash (right). The picture is based on the co-crystal structure (PDB Code 4FN5).

Fig. S7. Substrate specificity of the A4 domain of the argyrin NRPS. Observed mass shifts in deconvoluted protein MS TICs reveal loading of D-alanine (C) and D-serine (E) onto the PCP. L-alanine (B), L-serine (D) and glycine (F) were not accepted by the A-PCP (control: A).

Fig. S8. Increase in absorbance relative to the control (protein without amino acid) after the malachite green assay reactions incubated at 30°C for 1 h (left) and overnight at room temperature (right).

Table S1. List of primers used in this study.

Table S2. Gene synthesis constructs obtained from ATG: biosynthetics GmbH.

Table S3. Constructs generated in this study.

Table S4. Abbreviated and full names of the *M. xanthus* mutants generated in this study.

Table S5. HPLC-MS data of argyrin derivatives detected in the heterologous expression strains. Above the bold line are previously described derivatives and below the line are their methylated (R3=CH_3) counterparts newly detected in this study.